

# INTERNATIONAL SOCIETY FOR SOIL MECHANICS AND GEOTECHNICAL ENGINEERING



*This paper was downloaded from the Online Library of the International Society for Soil Mechanics and Geotechnical Engineering (ISSMGE). The library is available here:*

<https://www.issmge.org/publications/online-library>

*This is an open-access database that archives thousands of papers published under the Auspices of the ISSMGE and maintained by the Innovation and Development Committee of ISSMGE.*

*The paper was published in the proceedings of the 7<sup>th</sup> International Conference on Earthquake Geotechnical Engineering and was edited by Francesco Silvestri, Nicola Moraci and Susanna Antonielli. The conference was held in Rome, Italy, 17 - 20 June 2019.*

# Damage mechanism of reinforced concrete piles with axial load variation based on E-Defense shaking table tests

K. Shibata, H. Funahara & T. Nagao  
*Taisei Corporation, Kanagawa, Japan*

Y. Kawamata  
*National Research Institute for Earth Science and Disaster Resilience, Hyogo, Japan*

S. Tamura  
*Tokyo Institute of Technology, Tokyo, Japan*

**ABSTRACT:** A series of shaking table tests were conducted to investigate the bending-induced damage mechanism of piles using the world largest shaking table, “E-Defense” facility. Bending behaviors of reinforced concrete piles significantly depend on axial load acting on the piles. As a result of the tests, the following conclusions have been drawn. (1) Near the pile heads, the back side of the leading row piles tends to significantly suffer concrete compressive crushing because the compressive stress due to the pile bending and the pushdown load from the overturning of the superstructure are generated simultaneously. (2) Around the boundary between medium dense and dense sand layers, the back side of the trailing row piles tends to significantly suffer concrete tensile cracking and rebar yielding because the tensile stress due to the pile bending and the uplift load from the overturning of the superstructure are generated simultaneously.

## 1 INTRODUCTION

During the 1995 Hyogo Ken Nanbu Earthquake, many reinforced concrete (RC) piles were damaged. Most of them were damaged by ground liquefaction (Tokimatsu & Asaka 1998), but some were due to inertia force from their superstructures (Editorial Committee for the Report on the Hanshin-Awaji Earthquake Disaster 1998). Thus, the RC piles were damaged not only in the liquefied ground inducing significant deformation but also in non-liquefied ground.

When RC piles are subjected to lateral seismic loads, bending moment is generated along the piles. However, the bending strength of the RC piles depends on the axial load because concrete gives larger and less strength in compression and tension, respectively. The axial load along the piles keeps changing as overturning moment of their superstructure varies during an earthquake, and therefore, the bending properties of the piles are considerably inconstant. Because of this, it is essential to consider the change of bending strength for evaluation of the pile responses. It is important to adequately evaluate the influence of the axial load variation especially for structures with large aspect ratio such as high-rise buildings.

The seismic performance of RC piles has been investigated using large shaking table tests. The seismic behaviors of RC pile groups in saturated sand (Tamura & Hida 2009 and Yasuda et al. 2000) and in dry sand (Funahara et al. 2007) were investigated. Although Funahara et al. (2007) studied the influence of the axial load variation of the piles, experimental studies for this influence are relatively few. Therefore, further accumulation of the data is required.

Considering the above, shaking table tests were conducted to investigate effects of the axial load on RC pile damage mechanism using the large shaking table of 3-D Full-Scale Earthquake Testing Facility E-Defense at the Hyogo Earthquake Engineering Research Center of the National Research Institute for Earth Science and Disaster Resilience. Through the tests, a large number of valuable data on seismic behaviors of RC piles were obtained.

## 2 OUTLINE OF TEST PROGRAM

### 2.1 Test model and instruments

Outline of the test model is shown in Figure 1. Ground model was made by pouring two types of sand into a large laminar container with a diameter of 8 m and a height of 6.5 m. Two types of pile group models, a 3×2 RC pile group and a 3×3 steel pipe pile group, were installed in parallel to the main shaking direction (Y-direction) before putting the sand. The RC piles were designed to be damaged and the steel pipe piles were designed to remain into the elastic domain during a large earthquake motion. Sensors such as accelerometers, laser displacement transducers, strain gauges and earth pressure meters were installed to measure the dynamic behaviors of the model during the shaking tests. In this paper, behaviors of the RC pile group model are mentioned, and discussion on the steel pile group is described in Tamura et al. (in press). Sensor arrangements related to the RC pile group and surrounding soil are shown in Figures 1 and 2.

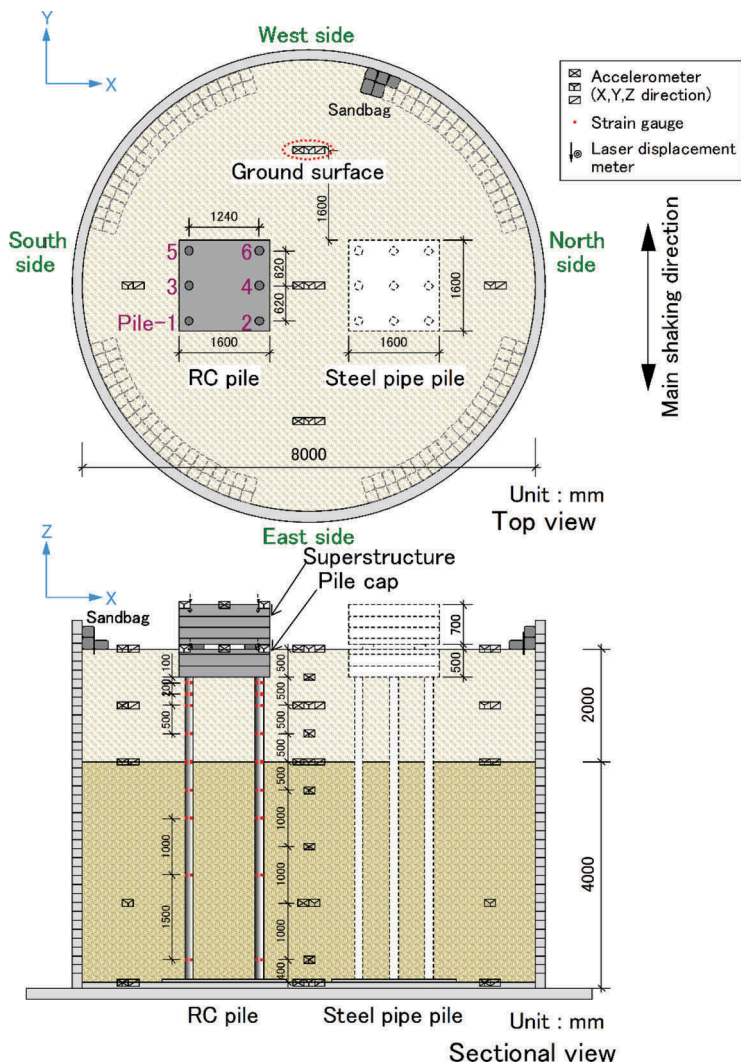


Figure 1. Outline of test model and sensor arrangements.

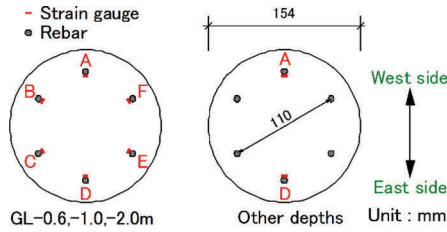


Figure 2. Strain gauge arrangements.

Table 1. Physical properties of ground.

Depth		Relative density	Dry density	Moisture content	Soil particle density	Maximum dry density	Minimum dry density	Mean grain size
	Ground material	%	g/cm <sup>3</sup>	%	g/cm <sup>3</sup>	g/cm <sup>3</sup>	g/cm <sup>3</sup>	mm
0–2	Kakezu sand	60.0	1.433	0.0	2.675	1.555	1.283	0.20
2–5.9	Albany sand	76.1	1.661	3.7	2.666	1.727	1.479	0.27

## 2.2 Properties of test model

A structural model, which consisted of a superstructure (14,000 kg) and a pile cap (10,000 kg) made by assembling steel plates, was placed on each pile group. The superstructure and pile cap of each model were connected with four laminated rubbers. The pile cap had a height of 500 mm and was embedded in the ground up to the upper end. The primary natural period of the superstructure was approximately 0.12 s, and the primary natural period of the coupled soil-pile-structure system was approximately 0.23 s. These natural periods were evaluated from Fourier spectral ratios of the superstructure to the pile cap and the superstructure to the shaking table respectively during a small shaking (shown in Special Project for Reducing Vulnerability for Urban Mega Earthquake Disasters 2017).

The piles had a diameter of 154 mm and were made of mortar with the uniaxial compressive strength of 27.2 N/mm<sup>2</sup>. The main rebars had a diameter of 6 mm and the yield strength of 377 N/mm<sup>2</sup>, and the shear rebars were spirally formed with 2 mm hard steel wires at a pitch of 20 mm. The pile heads were rigidly connected to the pile cap and the pile tips were just in contact with the bottom plate of the laminar container. Details of the connections are shown in Special Project for Reducing Vulnerability for Urban Mega Earthquake Disasters (2017).

The ground consisted of two layers, a medium dense upper layer and a dense lower layer. The upper layer of 2 m was made of the dry Kakezu silica sand with a relative density of approximately 60 %, and the lower layer of 4 m was made of the wet Albany silica sand with a relative density of approximately 80 %. The physical properties of these sands are shown in Table 1. The primary natural period of the ground was estimated to be approximately 0.12 s from results of the small shaking.

## 2.3 Input motions

A series of shaking table tests were conducted for 3 days as shown in Table 2. The test specimen was excited by simulated earthquake motions and observed earthquake records with the maximum acceleration adjusted. The simulated earthquake motions for this series of experiments were developed as artificial seismic motions on the engineering bedrock for design of high-rise buildings and satisfied the acceleration response spectrum requirements given by the Japanese government. These motions called Kokuji motions are extraordinary rare ground motions assuming approximately a 500-years return period. Since the phase characteristics of

Table 2. List of input motions.

Date	Wave	Acceleration amplitude
		g
1st day	Kokuji (JMA Kobe NS, NS-EW) 10%	NS: 0.04, EW: 0.04
	Kokuji (JMA Kobe NS, NS-EW, NS-EW-UD) 20%	NS: 0.08, EW: 0.08, UD: 0.04
	Kokuji (Hachinohe NS) 20%	0.08
	Observed wave (JR Takatori EW) 10%	0.07
2nd day	Kokuji (JMA Kobe NS) 100%	0.39
	Observed wave (JR Takatori EW) 60%	0.40
3rd day	Sine wave (T=0.2, 0.25, 0.3, 0.3, 0.3, 0.4s)	0.10, 0.10, 0.10, 0.20, 0.41, 0.31
	Kokuji (JMA Kobe NS) 100%	0.39
	Kokuji (JMA Kobe NS) 150%	0.58

\* NS-EW: bi-directional shaking, NS-EW-UD: tri-directional shaking.

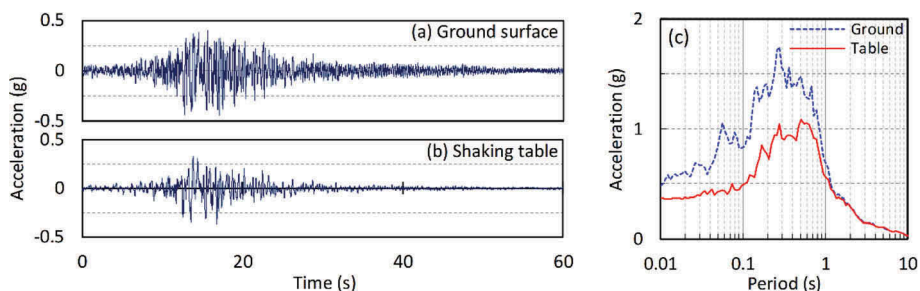


Figure 3. (a), (b) Acceleration time histories and (c) response spectra on ground surface and shaking table.

the Kokuji motions are not specifically defined by the government, a phase of a record observed at the Kobe Marine Observatory (JMA Kobe) during the 1995 Hyogo Ken Nanbu earthquake was applied in this study. In the 1st day, the acceleration amplitude of the input seismic motions was adjusted so as not to damage the piles, but to generate partial concrete cracks. In the 2nd and 3rd days, the acceleration amplitude of the input motions was increased to damage the piles more significantly.

In this paper, the cases of inputting the Kokuji motion (2nd day), in which axial strain along the rebars in the piles reached yielding strain for the first time, are described. The acceleration time histories and the acceleration response spectra on the ground surface and the shaking table are shown in Figure 3, respectively. Figure 3c shows that the spectrum at the ground surface was amplified up to a period of approximately 1.0 s, and the dominant period of the ground surface was approximately 0.3 s.

### 3 OVERVIEW OF TEST RESULTS

#### 3.1 Descriptions of time history graphs

Figure 4 shows the time histories of displacement of the pile cap and the ground surface, the structural inertia force, the axial load at 2.5 m below the pile top, the axial rebar strain at 0.1 m below the pile top and the shaking table acceleration. These figures show only from 10 to 25 s with remarkable responses. Piles-1, 4 and 5 are compared herein since the lead wires of the strain gauges were significantly damaged in Piles-2, 3 and 6. No remarkable twist was observed in the structural responses and strain gauge records in small shaking show that the behaviors of the pile group are almost symmetric with respect to the pile cap center line parallel to the shaking direction. Therefore, it can also be assumed that the adjacent piles in the orthogonal direction to the shaking were subjected to identical external force and subgrade reaction.

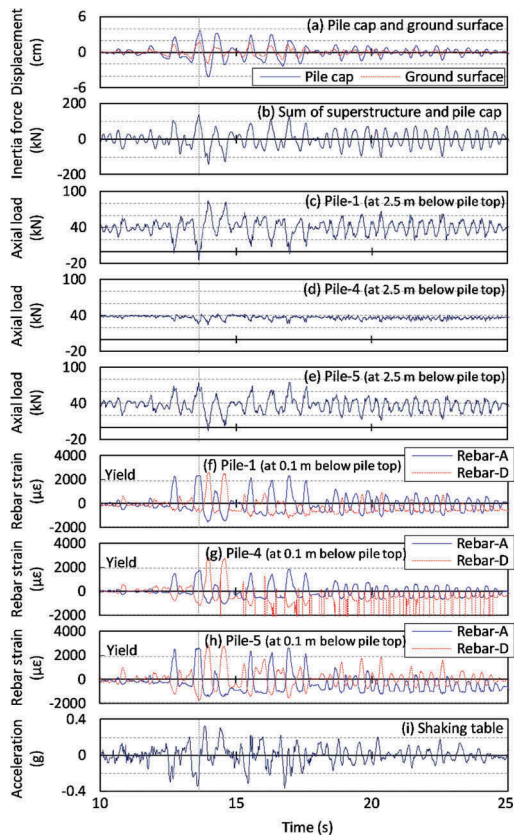


Figure 4. Time histories of (a) displacement at pile cap and ground surface, (b) inertia force, (c)-(e) axial load of piles, (f)-(h) rebar strain and (i) acceleration of shaking table.

### 3.2 Displacement of pile cap and ground surface

Figure 4a compares displacements of the pile cap and the ground surface. These displacements were evaluated as relative displacements of the pile cap and the ground surface with respect to the shaking table based on double integration of the accelerations. This figure shows that the displacement amplitude of the pile cap was larger than that of the ground surface. Because of this, it can be reasonably assumed that the inertial force of the superstructure was dominant to the dynamic behaviors of the piles for this test specimen. It is noted that additional studies on the kinematic effects to the pile behaviors are probably needed to obtain deeper understandings on the damage mechanism.

### 3.3 Time histories of inertia force

The inertia force in Figure 4b was evaluated by adding the contributions of the structural mass and of the pile cap mass. The maximum and minimum values of the inertia force appeared at around 14 s and were approximately 134.7 kN and -142.1 kN, respectively.

### 3.4 Time histories of axial load in piles

The axial loads in Figures 4c-e are evaluated as the sum of the variable axial load due to the shaking and the axial load due to the dead weight of the superstructure and the pile cap. The axial load variation has been calculated based on the rebar strain at the depth with no mortar crack. The initial axial load due to the dead weight has been evaluated by dividing the dead

weight of the superstructure and the pile cap by the number of the piles. It is assumed that the dead load has been supported only by the piles because the soil-pile cap contact has been released due to the vibration induced ground settlement in the previous excitations. The axial load variations during shaking calculated from the strain gauge records include redistribution of the dead weight as well as inertial effects from the superstructure and the pile cap.

The axial load variations were larger in the edge piles, the Piles-1 and 5 than the middle pile, Pile-4. This is because the edge piles mainly resist against the overturning moment of the superstructure. Furthermore, the axial load varied only toward the tensile side in the middle pile as shown in Figure 4d. This implies that the rotation axis of the rocking motion horizontally shifted from the center to the leading row pile side. This phenomenon probably occurred because the mortar cracking and the rebar yielding induced significant reduction of the pile stiffness in tension, and the pile tops tended to move upward more.

### 3.5 Time histories of rebar strain

Time histories of strains along the rebars in the piles are shown in Figures 4f-h, in which the horizontal dotted lines represent strain at rebar yielding. Due to the bending deformation of the piles, the strain of Rebars-A and D in all the piles are out-of-phase to each other. Each strain was significantly varied toward the tensile side, and the rebars yielded. Waveform disturbance observed on the data of Rebar-D of Pile-4 is probably due to measurement error.

## 4 PILE DAMAGE MECHANISM AFFECTED BY AXIAL LOAD VARIATION

### 4.1 Visual confirmation of pile damage

The visual inspection of the piles was performed at removal of the ground. The sketches of the cracks along the piles are shown in Figure 5. It should be noted that the crack conditions in this figure include the influence of larger shakings applied after the Kokuji motion in the 2nd day.

Many horizontal cracks due to the bending deformation were observed at shallower depths than the boundary of the two sand layers, 1.5 m below the pile top. The crack width tended to

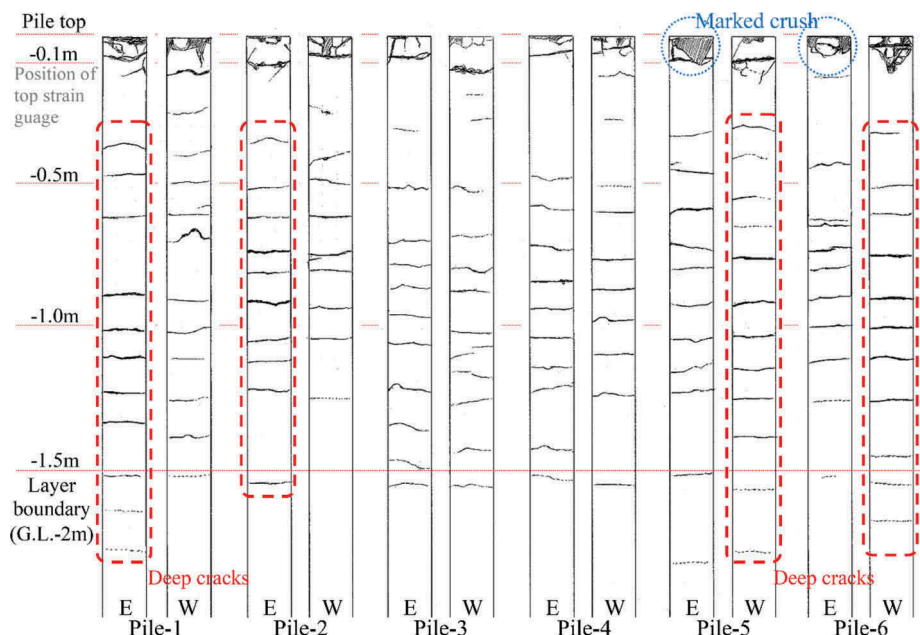


Figure 5. Sketches of cracks on RC piles.



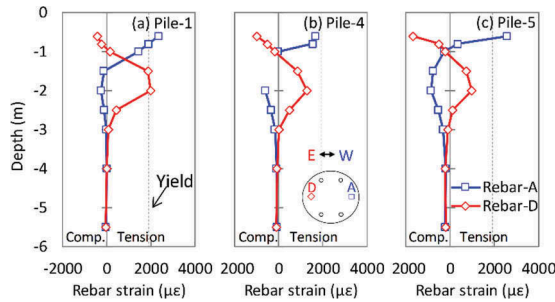


Figure 6. Profiles of rebar strain.

be large on the side facing to the free field, that is, on the east side of Piles-1, 2 and the west side of Piles-5, 6. In addition, the crush of the concrete was observed around the pile head and was more remarkable on the east side of Piles-5, 6 than elsewhere. An explanation of why Piles-5, 6 suffered more severe damages than Piles-1, 2 is the progressive accumulation of permanent horizontal displacements of the structural mass toward the west side recorded during the Kokuji motion (2nd and 3rd days) and the sine waves (3rd day).

#### 4.2 Profiles of rebar strain

Figure 6 shows the profiles of the strain on Rebars-A, D at the time when the maximum inertia force of the structure appeared. The maximum inertia force was observed at 13.620 s as shown with vertical dotted lines in Figure 4. Since the inertia force acted westward, Pile-5 was compressed and Pile-1 was extended. The data at G.L. -1.5 m along Rebar-A of Pile-4 is excluded from Figure 6 due to measurement failure.

The compressive strain was generated in Rebar-D (east side) around all the pile heads. Pile-5 was compressed more than Piles-1, 4 because the compressive strain along Rebar-D of Pile-5 included compressive strain due to the pile bending and pushdown load from the overturning of the superstructure as shown in Figure 7. On the contrary, since Rebar-D of Pile-1 was subjected to uplift load from the overturning of the superstructure, the compressive strain became smaller. Therefore, the back side of the leading row piles tended to significantly suffer concrete compressive crushing near the pile heads.

On the other hand, the tensile strain was generated in Rebar-A (west side) around each pile head. Comparing the strain profiles along Pile-1 to Pile-5, the tensile strains at G.L. -0.6 m were almost the same, but, at larger depth, the tensile strains attained along Pile-1 overcome those along Pile-5. This is because tensile strain due to uplift load from the superstructure as well as bending strain were generated on Rebar-A of Pile-1 simultaneously. The tensile strain of Pile-5 at G.L. -0.6 m was considerably large, despite the axial compressive load acting on the head of this pile. This is probably because cracking occurred in the mortar at the attachment depth of the strain gauge.

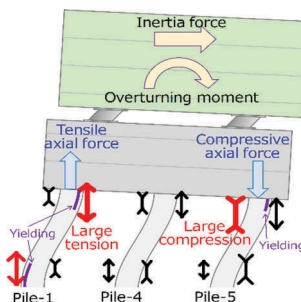


Figure 7. Situation of test model.



In addition, the tensile strain at G.L. -2 m was generated in Rebar-D, because the direction of the bending moment at this depth was opposite to that at the pile heads. The uplift load from the overturning of the superstructure acting along Pile-1 contributed to the larger tensile strain of Rebar-D in Pile-1 than in Piles-4, 5 and it resulted in yielding of Rebar-D in Pile-1 around G.L. -2 m. As a result, the back side of the trailing row piles tended to significantly suffer concrete tensile cracking and rebar yielding around this depth.

## 5 CONCLUSIONS

The shaking table tests in E-Defense facility with the 3×2 RC pile group were conducted to investigate the influence of the axial load variation on the pile damage. As a result, the following conclusions have been obtained.

1. Near the pile heads, the back side of the leading row piles tends to significantly suffer concrete compressive crushing because the compressive stress due to the bending and the push-down load from the overturning of the superstructure are generated simultaneously.
2. Around the boundary between medium dense and dense sand layers, the back side of the trailing row piles tends to significantly suffer concrete tensile cracking and rebar yielding because the tensile stress due to the bending and the uplift load from the overturning of the superstructure are generated simultaneously.

## ACKNOWLEDGEMENTS

These tests in E-Defense facility are a part of “Special Project for Maintenance and Recovery of Functionality in Urban Infrastructures” sponsored by MEXT in Japan. All their supports are deeply appreciated.

## REFERENCES

- Editorial Committee for the Report on the Hanshin-Awaji Earthquake Disaster. 1998. Report on the Hanshin-Awaji Earthquake Disaster. Building Series Volume 4, Damage to Building Foundation (in Japanese)
- Funahara, H., Oishi, M., Tateishi, A., Hata, A. & Abe, A. 2007. Large-scale shaking table tests and numerical simulation on dynamic nonlinear behavior of reinforced concrete piles and dry sand deposits, The 4th U.S.-Japan Workshop on Soil-Structure-Interaction Tsukuba, Japan.
- Special Project for Reducing Vulnerability for Urban Mega Earthquake Disasters, (ii) Maintenance and Recovery of Functionality in Urban Infrastructures. 2017. Technical Report for Condition Assessment of Structures—Soils and Underground Structures (in Japanese)
- Tamura, S. & Hida, T. 2009. Effects of RC pile damage on structure behavior based on liquefaction tests using large scaleshear box, *Journal of structural and construction engineering (Transactions of AIJ)*, 74(635), 91–96. (in Japanese)
- Tamura, S., Ohno, Y., Shibata, K., Funahara, H., Nagao, T. & Kawamata, Y. in press. Lateral resistance of piles in a group under E-Defense shaking-table tests, (submitted to 7th International Conference on Earthquake Geotechnical Engineering)
- Tokimatsu, K. & Asaka, Y. 1998. Effects of liquefaction-induced ground displacements on pile performance in the 1995 Hyogoken-Nanbu earthquake, *Special issue of soils and foundations*, 163–177.
- Yasuda, S., Ishihara, K., Morimoto, I., Orense, R., Ikeda, M. & Tamura, S. 2000. Large-scale shaking table tests on pile foundations in liquefied ground, *Proceeding of the 12th World Conference on Earthquake Engineering (12WCEE)*, New Zealand, Paper 1474.